

Efficiency in Multivariate Functional Nonparametric Models with Autoregressive Errors

S. Dabo-Niang^{a,c}, S. Guillas^b, C. Ternynck^{a,*}

^aLaboratory LEM, University of Lille, Villeneuve-d'Ascq, France.

^bUniversity College London, London, United Kingdom.

^cModal team INRIA, Lille, France.

Abstract

In this paper, we introduce a new procedure for the estimation in the nonlinear functional regression model where the explanatory variable takes values in an abstract function space and the residual process is autocorrelated. Moreover, we consider the case where the response variable takes its values in \mathbb{R}^d , $d \geq 1$. The procedure consists in a pre-whitening transformation of the dependent variable based on the estimated autocorrelation. We establish both consistency and asymptotic normality of the regression function estimate. For kernel methods encountered in the literature, the correlation structure is commonly ignored (the so-called “working independence estimator”); we show here that there is a strong benefit in taking into account the autocorrelation in the error process. We also find that the improvement in efficiency can be large in our functional setting, up to 25% in the presence of high autocorrelation levels. We discover that the additional step of iterating the fitting process actually deteriorates the estimation. We illustrate the skills of the methods on simulations as well as on application on ozone levels over the US.

Keywords: Autoregressive process, Functional data, Kernel regression, Pre-whitening, Time Series

1. Introduction

The use of functional random variables is spreading in statistical analyses due to the availability of high frequency data and of new mathematical strategies to deal with such statistical objects. The field is known as Functional Data Analysis (FDA). Applications of FDA are growing across fields as diverse as energy studies (Antoniadis et al., 2014), linguistics (Aston et al., 2010), atmospheric chemistry (Park et al., 2013), and human vision (Ogden and Greene, 2010). The functional variables are mainly curves, but surfaces and manifolds are nowadays considered (e.g. Guillas and Lai, 2010; Sangalli et al., 2013). For an introduction to this field as well as illustrations and applications, see

*Corresponding author

Email addresses: `sophie.dabo@univ-lille3.fr` (S. Dabo-Niang), `s.guillas@ucl.ac.uk` (S. Guillas), `ternynck.camille@gmail.com` (C. Ternynck)

9 Ramsay and Silverman (2005). Besides, Ferraty and Vieu (2006) present nonparametric methods,
 10 suited to such functional regression, with a more mathematical flavor. More recently, Cuevas (2014)
 11 provides an updated survey of the state of the art in FDA theory.

12 Among the nonparametric functional regression methods, the kernel estimator is often used to
 13 estimate the regression operator. It yields almost sure consistency in the case of an independent
 14 sample (Ferraty and Vieu, 2002) or an α -mixing sample (Ferraty et al., 2002a,b), but also asymp-
 15 totic normality in the independent case (Ferraty et al., 2007) with exact computation of all the
 16 constants for its precise use in practice. Masry (2005) established the asymptotic normality of the
 17 nonparametric regression estimator for strongly mixing processes albeit with abstract expressions
 18 of the constants so this is more challenging to use in practice. Delsol (2007, 2009) generalized the
 19 results of Ferraty et al. (2007) to the case of an α -mixing dataset.

20 In this paper, we consider the regression of a multivariate random variable onto a functional
 21 random variable. The estimation of the regression function is tackled by means of a nonparametric
 22 kernel approach. The existing kernel regression estimators dealing with functional explanatory
 23 variables are for scalar response; we have not found existing research on functional nonparametric
 24 modeling for multivariate response. With multivariate explanatory variables and a multivariate
 25 response, Xiang et al. (2013) proposed a kernel estimate of the regression function. Our regression
 26 model below is an extension of (Xiang et al., 2013):

$$\mathbf{Y}_t = \mathbf{m}(X_t) + \mathbf{u}_t, \quad t = 1, \dots, T, \quad (1)$$

27 where $\mathbf{Y}_t = (Y_{t,1}, \dots, Y_{t,d})' \in \mathbb{R}^d$, $\mathbf{m}(X_t) = (m_1(X_t), \dots, m_d(X_t))'$, the explanatory vari-
 28 able is functional (that is, X_t takes values in some possibly infinite-dimensional space), $\mathbf{u}_t =$
 29 $(u_{t,1}, \dots, u_{t,d})'$. Moreover, the stationary residual process \mathbf{u}_t is autocorrelated and independent of
 30 X_t . We do not necessarily assume that $(X_t, \mathbf{Y}_t)_t$ is strictly stationary, second order stationarity
 31 suffices.

32 Although, for the kernel methods proposed in the literature, it is generally better to ignore the cor-
 33 relation structure entirely (the so-called “working independence estimator”, e.g. Ruckstuhl et al.
 34 (2000), Lin and Carroll (2000)), we show here that taking into account the autocorrelation of the
 35 error process helps improve the estimation of the regression function.

36 We extend the kernel-based procedure proposed by Xiao et al. (2003) for estimating $m(x)$ in the
 37 time series regression model for multivariate explanatory variables x to a functional setting. Xiao
 38 et al. (2003) showed that their procedure is more efficient than the conventional local polynomial
 39 method. The main idea is to transform the original regression model, so that this transformed
 40 regression has a residual term that is uncorrelated. This transformation depends on the func-
 41 tion $\mathbf{m}(\cdot)$ and on the parameters of the autoregressive representation of \mathbf{u} , since the regression
 42 function is nonlinear. The error correlation structure is assumed to have an autoregressive repre-
 43 sentation. Firstly, the parameters of the autoregressive representation are estimated. In a second

44 step, a transformation $\widehat{\mathbf{Y}}_t$ of the dependent variable \mathbf{Y}_t is constructed by plugging in the estimated
 45 autocorrelation parameter. Finally, the estimation of \mathbf{m} is carried out on this filtered series $\widehat{\mathbf{Y}}_t$.

46 The remainder of the paper is organized as follows. In Section 2, we introduce the estimation
 47 method as well as the assumptions. We then provide asymptotic results for the estimator proposed.
 48 Section 3 is devoted to a simulation case study and an illustration of our method for ozone levels
 49 over the US. The conclusion is done in Section 4 while the proofs are given in the Appendix.

50 2. Assumptions and main results

51 Suppose that we have a sample $\{(X_1, \mathbf{Y}_1), \dots, (X_T, \mathbf{Y}_T)\}$, where $X_t, t = 1, \dots, T$, is a random
 52 variable taking its values in a semi-metric space (\mathcal{C}, d) of infinite dimension and $\mathbf{Y}_t \in \mathbb{R}^d$ is the
 53 response from the nonparametric regression (1). We assume that the residual process $\mathbf{u}_t \in \mathbb{R}^d$ is
 54 stationary, has mean $\mathbf{0}$ with cross-covariance (auto-covariance in the univariate case) $\gamma_{\mathbf{u}}$ and has
 55 the following invertible linear process representation (with bounded coefficients):

$$\mathbf{u}_t = \sum_{k=0}^{\infty} \Psi_k \mathbf{e}_{t-k} = \Psi(L) \mathbf{e}_t \quad (2)$$

56 where $\Psi_0 = I$ (identity matrix), $\Psi(L) = \sum_{k=0}^{\infty} \Psi_k L^k$ is a $d \times d$ matrix in the lag operator L
 57 ($L^k(\mathbf{e}_t) = \mathbf{e}_{t-k}$), the (i, j) th element of $\Psi(L)$ is $\psi_{ij}(L) = \sum_{k=0}^{\infty} c_{ij}(k) L^k$, the $\mathbf{e}_t \in \mathbb{R}^d$ form a white
 58 noise process with mean $\mathbb{E}(\mathbf{e}_t) = \mathbf{0}$, $\mathbb{E}(\mathbf{e}_t \mathbf{e}_t') = \Sigma_{\mathbf{e}}$ is a positive definite matrix, $\mathbb{E}(\mathbf{e}_t \mathbf{e}_{t+k}) = \mathbf{0}$ for
 59 $k \neq 0$ and $\mathbb{E}[|e_{t,j}|] < \infty, \forall j = 1, \dots, d$.

60 Let $\Psi(L)^{-1} = \Pi(L) = I - \sum_{k=1}^{\infty} \Pi_k L^k$ with $\Pi_0 = I$, or as done for Ψ let the (i, j) th element of
 61 $\Pi(L)$ be $\pi_{ij}(L) = \sum_{k=0}^{\infty} a_{ij}(k) L^k$. So we have, the infinite autoregressive representation

$$\Pi(L) \mathbf{u}_t = \mathbf{e}_t. \quad (3)$$

62 Note that stationary, causal and invertible vector ARMA processes $\mathbf{u}_t - \sum_{k=1}^p \Phi_k \mathbf{u}_{t-k} = \mathbf{e}_{t-k} -$
 63 $\sum_{k=1}^q \Theta_k \mathbf{e}_{t-k}$ can be represented as in (2)-(3) if all roots of $\det\{\Phi(L)\}$ and $\det\{\Theta(L)\}$ are all greater
 64 than one in absolute value.

65 Here, we consider a truncated version of $\Pi(L)$ at order Q , that is $\Pi(L) = I - \sum_{k=1}^Q \Pi_k L^k$, where
 66 the truncation parameter Q is large enough. Applying $\Pi(L)$ to the regression in Equation (1), we
 67 obtain $\Pi(L) \mathbf{Y}_t = \Pi(L) \mathbf{m}(X_t) + \mathbf{e}_t$. Then let the regression model $\underline{\mathbf{Y}}_t = \mathbf{m}(X_t) + \mathbf{e}_t$, with $\underline{\mathbf{Y}}_t =$
 68 $\mathbf{Y}_t - \sum_{k=1}^Q \Pi_k L^k (\mathbf{Y}_t - \mathbf{m}(X_t))$, so the error term in this transformed model is now uncorrelated.
 69 The matrix of coefficients $\{\Psi_k\}_{k=0}^{\infty}$ and the regression function $\mathbf{m}(\cdot)$ are unknown, except for the
 70 fact that $\mathbf{m}(\cdot)$ is a smooth function. If $\underline{\mathbf{Y}}_t$ were known then a nonparametric kernel regression of $\underline{\mathbf{Y}}_t$
 71 on X_t would be more efficient than the conventional kernel estimation. In this work, we employ a
 72 Nadaraya-Watson estimator as introduced in Ferraty and Vieu (2004), Masry (2005), Dabo-Niang
 73 and Rhomari (2009) where for any sample $\{V_t, X_t\}$, the estimation of the regression of $V_t \in \mathbb{R}$ onto
 74 $X_t \in (\mathcal{C}, d(\cdot, \cdot))$ is

$$\frac{\sum_{t=1}^T V_t K\left(\frac{d(x, X_t)}{h}\right)}{\sum_{s=1}^T K\left(\frac{d(x, X_s)}{h}\right)}, \quad x \in \mathcal{C}$$

75 where $K(\cdot)$ is a function over $[0, +\infty[$ called kernel, $h > 0$ is the bandwidth parameter and $d(\cdot, \cdot)$
76 is a semi-metric. For $x \in \mathcal{C}$ fixed, let $\hat{m}_j(x)$ be the corresponding estimator with $V_t = Y_{t,j}$ and let
77 $\bar{m}_j(x)$ be the corresponding estimator when $V_t = \underline{Y}_{t,j}$. Let K_0 and K_1 be two kernels over $[0; +\infty[$,
78 h_0 and h_1 the two corresponding bandwidths. Consider the estimator $\bar{\mathbf{m}}(x) = (\bar{m}_1(x), \dots, \bar{m}_d(x))'$
79 where

$$\bar{m}_j(x) = \frac{\frac{1}{T\mathbb{E}\left[K_0\left(\frac{d(x, X_1)}{h_0}\right)\right]} \sum_{t=1}^T Y_{t,j} K_0\left(\frac{d(x, X_t)}{h_0}\right)}{\frac{1}{T\mathbb{E}\left[K_0\left(\frac{d(x, X_1)}{h_0}\right)\right]} \sum_{s=1}^T K_0\left(\frac{d(x, X_s)}{h_0}\right)} = \frac{\bar{m}_{2,j}(x)}{\bar{m}_1(x)}, \quad j = 1, \dots, d$$

80 In practice, the matrix of coefficients $\{\Pi_k\}_{k=1}^Q$ is unknown and therefore $\underline{\mathbf{Y}}_t$ is not computable,
81 so the regression $\underline{\mathbf{Y}}_t = \mathbf{m}(X_t) + \mathbf{e}_t$ and $\bar{\mathbf{m}}(x)$ are unworkable. A feasible estimator is obtained
82 by replacing $\underline{\mathbf{Y}}_t$ by its approximation based on estimates of $\{\Pi_k\}_{k=1}^Q$. The proposed estimation
83 procedure extends Xiao et al. (2003).

- 84 1. For $j = 1, \dots, d$: obtain a preliminary consistent estimate of \mathbf{m} by the regression of \mathbf{Y}_t on X_t
85 with corresponding kernel K_0 and bandwidth h_0 assuming i.i.d. errors. Denote the preliminary
86 estimate as $\hat{\mathbf{m}}(X_t)$ and calculate the estimated residuals $\hat{\mathbf{u}}_t = \mathbf{Y}_t - \hat{\mathbf{m}}(X_t)$, $\hat{\mathbf{u}}_t = (u_{t,1}, \dots, u_{t,d})'$,
87 $\hat{u}_{t,j} = Y_{t,j} - \hat{m}_j(X_t)$.
- 88 2. Conduct an estimation of the $VAR(Q)$ matrix coefficients in the autoregression of $\hat{\mathbf{u}}_t$: $\hat{\mathbf{u}}_t =$
89 $\hat{\Pi}_1 \hat{\mathbf{u}}_{t-1} + \dots + \hat{\Pi}_Q \hat{\mathbf{u}}_{t-Q} + \mathbf{e}_t$, where $\mathbf{e}_t = (e_{t,1}, \dots, e_{t,d})'$ is a vector of i.i.d. noise.
- 90 3. Construct an approximation of $\underline{\mathbf{Y}}_t$, $t = 2, \dots, T$ that is $\hat{\underline{\mathbf{Y}}}_t = \mathbf{Y}_t - \hat{\Pi}_1 (\mathbf{Y}_{t-1} - \hat{\mathbf{m}}(X_{t-1})) - \dots -$
91 $\hat{\Pi}_Q (\mathbf{Y}_{t-Q} - \hat{\mathbf{m}}(X_{t-Q}))$. The proposed estimator of $\mathbf{m}(x)$ is then obtained from the regression
92 of $\hat{\underline{\mathbf{Y}}}_t$ on X_t with corresponding kernel K_1 and bandwidth h_1 , resulting in the estimator $\tilde{\mathbf{m}}(x) =$
93 $(\tilde{m}_1(x), \dots, \tilde{m}_d(x))'$:

$$\tilde{m}_j(x) = \frac{\frac{1}{T\mathbb{E}\left[K_1\left(\frac{d(x, X_1)}{h_1}\right)\right]} \sum_{t=2}^T \hat{Y}_{t,j} K_1\left(\frac{d(x, X_t)}{h_1}\right)}{\frac{1}{T\mathbb{E}\left[K_1\left(\frac{d(x, X_1)}{h_1}\right)\right]} \sum_{s=2}^T K_1\left(\frac{d(x, X_s)}{h_1}\right)}$$

94 For simplicity, let $Q = 1$ in the following. The proofs and results remain similar in the general
95 case $Q > 1$. Note that one can iterate this process, in case the initial estimate of the autocorrelation

96 is not accurate enough as the bias in this estimate will propagate to the filtered series and hence
 97 to the estimation of $\mathbf{m}(x)$. In our numerical studies, we present both the initial estimate and the
 98 estimate based on an additional iteration of the steps above.

99 Let us now explain in details the theoretical set-up that enables us to prove the asymptotic
 100 results in our paper. We first assume that the error process $\{\mathbf{u}_t\}$ is independent of the process $\{X_t\}$
 101 and that $\mathbb{E}[\mathbf{e}_t|X_t] = 0$. We consider that the processes $\{X_t, \mathbf{Y}_t\}$ are α -mixing, the most general
 102 case of weakly dependent variables. Let \mathcal{F}_a^b be the σ -algebra of events generated by the random
 103 variables $\{X_t, \mathbf{Y}_t\}_{t=a}^b$ and set (Rosenblatt (1956))

$$\sup_{A \in \mathcal{F}_{-\infty}^0, B \in \mathcal{F}_k^\infty} |\mathbb{P}(A \cap B) - \mathbb{P}(A)\mathbb{P}(B)| = \alpha(k) \xrightarrow{k \rightarrow \infty} 0.$$

104 Let $|\cdot|$ denote the L_1 -norm when it is applied to a vector; $|\mathbf{y}| = \sum_{j=1}^d |y_j|$, $\mathbf{y} = (y_1, \dots, y_d)'$
 105 and the usual matrix norm when applied to a matrix.

106 Our assumptions are listed below:

107 **H1** (*Smoothness*)

- 108 (1) $m_j(\cdot)$ is a bounded Lipschitz function: $|m_j(u) - m_j(v)| \leq c_3 d(u, v)^\beta$ for all $u, v \in (\mathcal{C}, d)$
 109 for some $\beta > 0$.
 110 (2) Let $\mathbf{G}_2(u) = \text{Var}[\mathbf{Y}_t|X_t = u]$, $u \in (\mathcal{C}, d)$, the variance matrix of \mathbf{Y}_t given $X_t = u$.
 111 $\mathbf{G}_2(u)$ is independent of t and is continuous in some neighborhood of x

$$\sup_{\{u: d(x, u) \leq h\}} |\mathbf{G}_2(u) - \mathbf{G}_2(x)| = o(1) \quad \text{as } h \rightarrow 0$$

112 Assume $\mathbb{E}|\mathbf{Y}_t|^\nu < \infty$ and $\mathbb{E}|\mathbf{e}_t|^\nu < \infty$, for some $\nu > 2$. Assume

$$\mathbf{G}_\nu(u) = \mathbb{E}[|\mathbf{Y}_t - \mathbf{m}(x)|^\nu | X_t = u], u \in (\mathcal{C}, d)$$

113 is continuous in some neighborhood of x .

- 114 (3) Define

$$\mathbf{G}(u, v; x) = \mathbb{E}[(\mathbf{Y}_t - \mathbf{m}(x))(\mathbf{Y}_s - \mathbf{m}(x)) | X_t = u, X_s = v], \quad t \neq s \text{ and } u, v \in (\mathcal{C}, d)$$

115 Assume that $\mathbf{G}(u, v; x)$ does not depend on t, s and is continuous in some neighborhood
 116 of (x, x) .

117 **H2** (*Kernel*) The kernels K_i , $i = 0$ or 1 , are symmetric nonnegative bounded kernels with compact
 118 support $[0, 1]$ satisfying

- 119 (1) $\int K_i(u) du = 1$ and $c_{1,i} \mathbf{1}_{[0,1]} < K_i < c_{2,i} \mathbf{1}_{[0,1]}$, $c_{1,i}$ and $c_{2,i}$ are two finite constants.

120 (2) For $j = 1, 2$, we have $I_j(h) \rightarrow C_j$ as $h \rightarrow 0$, for some positive constant C_j , with

$$I_j(h) = \frac{1}{\phi(h)/h} \int_0^1 K_i^j(u) \phi'(hv) dv \quad \text{where } \phi(\cdot) \text{ is defined below.}$$

121 Let $\mathcal{B}(x, h)$ be a ball centered at $x \in (\mathcal{C}, d)$ with radius h and let f_k , $k = 1, 2$ and 3 , be
 122 finite nonnegative functionals. Finally, we introduce the following notations, where $F_x^t(h)$
 123 corresponds to the well-known notion of small ball probabilities (see e.g. Dabo-Niang (2004),
 124 Ferraty and Vieu (2006)):

$$\begin{aligned} F_x^t(h) &= \mathbb{P}[X_t \in \mathcal{B}(x, h)] && := \mathbb{P}[d(X_t, x) \leq h] \\ F_{x,x}^{s,t}(h) &= \mathbb{P}[(X_t, X_s) \in \mathcal{B}(x, h) \times \mathcal{B}(x, h)] && := \mathbb{P}[d(X_t, x) \leq h, d(X_s, x) \leq h] \\ F_{x,y}^{s,t}(h) &= \mathbb{P}[(X_t, X_s) \in \mathcal{B}(x, h) \times \mathcal{B}(y, h)] && := \mathbb{P}[d(X_t, x) \leq h, d(X_s, y) \leq h] \end{aligned}$$

125 **H3** (*Distributions*)

126 (1) $F_x^t(h) = \phi(h)f_1(x)$ as $h \rightarrow 0$, where $\phi(0) = 0$ and $\phi(h)$ is absolutely continuous in a
 127 neighborhood of the origin and $f_1(X_t)$ is uniformly bounded and bounded away from
 128 zero.

129 (2) $\sup_{t \neq s} F_{x,x}^{s,t}(h) \leq \psi_1(h)f_2(x)$ as $h \rightarrow 0$, where $\psi_1(h) \rightarrow 0$ as $h \rightarrow 0$ and $f_2(X_t) < \infty$ is
 130 uniformly bounded and bounded away from zero.

131 Assume that the ratio $\psi_1(h)/\phi^2(h)$ is bounded. It is also supposed that $\exists \zeta_1 \in (0, 1)$,
 132 $0 < F_{x,x}(h) = O(\phi(h)^{1+\zeta_1})$.

133 (3) $\sup_{t \neq s} F_{x,y}^{s,t}(h) \leq \psi_2(h)f_3(x, y)$ as $h \rightarrow 0$, where $\psi_2(h) \rightarrow 0$ as $h \rightarrow 0$ and $f_3(X_t, X_s) < \infty$
 134 is uniformly bounded and bounded away from zero.

135 Assume that the ratio $\psi_2(h)/\phi^2(h)$ is bounded.

136 **H4** (*Mixing*) $\sum_{l=1}^{\infty} l^\delta [\alpha(l)]^{1-2/\nu} < \infty$

137 for some $\nu > 2$ and $\delta > 1 - 2/\nu$. Note that ν is the order of the moment in **H1**(2).

138 **H5** Let $h_i \rightarrow 0$, $h_0/h_1 \rightarrow 0$ and $\frac{\log T}{T^{1/2}\phi(h_0)} \rightarrow 0$ as $T \rightarrow \infty$. Let $\{v_T\}$ be a sequence of positive
 139 integers satisfying $v_T \rightarrow \infty$ such that $v_T = o((T\phi(h_0))^{1/2})$ and $(T/\phi(h_0))^{1/2}\alpha(v_T) \rightarrow 0$,
 140 $Th_0^{2\beta} \rightarrow 0$ as $T \rightarrow \infty$.

141 **Remark 1.**

142 - Hypothesis **H1**(1) is a mild smoothness assumption for kernel functions in nonparametric es-
 143 timation whereas hypotheses **H1**(2) and **H1**(3) are continuity assumptions on certain second-
 144 order moments.

145 - Hypothesis **H2**(1) on the kernel is standard. From hypothesis **H2**(2), if the kernel K_i satisfies
 146 $0 < c_1 \leq K_i(t) \leq c_2 < \infty$, then $c_1 \leq I_j(h) \leq c_2$. In fact, this assumption yields an expression
 147 of the asymptotic variance (rather than upper and lower bounds).

148 - Hypotheses of type **H3** were proposed in Masry (2005) and have been motivated by the work of
 149 Gasser et al. (1998). These hypotheses are linked to the volume of an n -ball. When $X \in \mathbb{R}^d$,
 150 $f_1(x)$ refers to the probability density of the random variable X and $\phi(h)$ is the volume of the
 151 unit ball in \mathbb{R}^d . Assumptions **H3**(2) and **H3**(3) concern the behavior of joint distribution.

152 - Hypothesis **H4** is a standard assumption on the decay of the strongly mixing coefficient $\alpha(l)$
 153 and hypothesis **H5** concerns the rate of the decay of the mixing coefficient.

154 Let $\Delta_t^{(i)}(x) = K_i\left(\frac{d(x, X_t)}{h_i}\right)$, $\mathbf{Z}_t^{(i)}(x) = [\mathbf{Y}_t - \tilde{\mathbf{m}}(x)]\Delta_t^{(i)}(x) - \mathbb{E}\left[(\mathbf{Y}_t - \tilde{\mathbf{m}}(x))\Delta_t^{(i)}(x)\right]$, for
 155 $i = 0, 1$ (see below). In the following, \xrightarrow{d} denotes the convergence in distribution. The following
 156 theorem gives the asymptotic normality of the estimator $\tilde{\mathbf{m}}(x)$ based on the transformation of the
 157 dependent variable.

Theorem 1. Under assumptions **H1-H5**, we have

$$(T\phi(h_1))^{1/2}[\tilde{\mathbf{m}}(x) - \mathbf{m}(x) - \mathbf{B}_T(x)] \xrightarrow{d} \mathcal{N}_d(0, \Sigma_x)$$

158 with $\mathbf{B}_T(x) = \mathbb{E}[\tilde{\mathbf{m}}(x)] - \mathbf{m}(x)$, $\Sigma_x = \frac{C_2 \mathbf{G}_2(x)}{C_1^2 f_1(x)} = \lim_{T \rightarrow \infty} \frac{\phi(h_1) \text{Var}(\mathbf{Z}_T^{(1)}(x))}{\mathbb{E}^2(\Delta_1^{(1)}(x))}$ is the $(d \times d)$ asymptotic
 159 covariance matrix, $x \in (\mathcal{C}, d)$ whenever $f_1(x) > 0$.

160 The following theorem gives a consistency result of the estimator $\tilde{\mathbf{m}}(x)$.

161 **Theorem 2.** Under assumptions **H1-H5**,

$$\lim_{T \rightarrow \infty} \tilde{\mathbf{m}}(x) = \mathbf{m}(x) \quad \text{in probability.}$$

162 **Remark 2.** One can establish a convergence in probability of $\tilde{\mathbf{m}}(x)$ with rate (for instance assum-
 163 ing for simplicity the boundedness of the response, even though the bound can be arbitrarily large)
 164 and state that:

$$|\tilde{\mathbf{m}}(x) - \mathbf{m}(x)| = O_p(h_0^\beta) + o_p\left(\sqrt{\frac{1}{T\phi(h_1)}}\right)$$

165 under conditions of Theorem 2.

166 The proofs of these theorems are postponed in the Appendix section.

167 3. Numerical results

168 3.1. Simulation study

169 We investigate the proposed estimator on simulated data, considering first the univariate case
 170 ($d = 1$). The functional observations X_t (with $t = 1, \dots, T$) are defined by $X_t(w) = 1 + 10e_{0,t} +$

171 $3e_{1,t}w^2 + 4e_{2,t}(1-w)^3$, $w \in [0, 1]$ where $e_{0,t}$, $e_{1,t}$ and $e_{2,t}$ are i.i.d. $\mathcal{N}(0, 1)$. We take $m(X_t(w)) =$
172 $\sqrt{|0.5 \int_0^1 X_t(w)dw|}$. The error process u_t is an $AR(1)$ process, that is $u_t = \epsilon_t + \rho\epsilon_{t-1}$ where ϵ_t
173 are i.i.d. $\mathcal{N}(0, \sigma = 1)$. Various values of ρ are considered. The number of replications is 200.
174 We report the relative efficiency (denoted as RE) calculated as the ratio of squared errors. Table
175 1 describes summary statistics of the relative efficiency for $T = 200$ whereas Table 2 gives the
176 average of the relative efficiency for different values of T . $RE1$ reports the relative efficiency of
177 the proposed efficient estimator $\tilde{m}(x)$ over the conventional estimator $\hat{m}(x)$, and $RE2$ concerns
178 the relative efficiency of the iterated estimator, over $\hat{m}(x)$. We did not implement the efficient
179 estimator of Xiao et al. (2003) as we only consider here for simplicity the case of one lag, but
180 the efficient estimator could be used in our context with larger lags than one. Instead here we
181 report results about the iterated estimates. The semi-metric $d(\cdot, \cdot)$ for computing proximities
182 between curves X_t plays a major role and depends on the specified statistical problem and dataset.
183 After trying some semi-metrics which can select most of the pertinent information of the curves,
184 we choose $d(\cdot, \cdot)$ inside the family of principal component semi-metrics (see Ferraty and Vieu
185 (2006)) which is defined by $d_q^{PCA}(X_t, X) = \sqrt{\sum_{k=1}^q (\int [X_t(w) - X(w)]v_k(w)dw)^2}$ where v_1, v_2, \dots
186 are the orthonormal eigenfunctions of the covariance operator and q is a tuning parameter. We
187 have considered different values for this parameter q and the value of 1 is better suited to this
188 simulation study. This number of principal components allows to explain around 98% of variation
189 of the curves. This choice for the semi-metric based on principal components is well adapted to
190 the considered polynomial functions X we deal with and for which it is important to take into
191 account large variations of the data. Regarding the implementation of the estimators, we use the
192 quadratic kernel (Epanechnikov) (defined by $K(x) = \frac{3}{4}(1-x^2)\mathbf{1}_{[-1;+1]}(x)$). Another choice to
193 make is the bandwidth parameters. It is well known that the performance of the kernel estimate
194 depends on the choice of the window parameter. The bound in Remark 2 allows us to choose the
195 window parameters that minimize this bound. This choice of the bandwidths leads to be optimal
196 in the finite dimensional case. In practice, a useful bandwidth choice method is cross-validation as
197 follows. For instance, cross-validation ideas are encountered in the finite dimensional setting (e.g.
198 Hardle and Marron (1985), Hart and Vieu (1990)) as well as on the infinite dimensional one (e.g.
199 Rachdi and Vieu (2007), Benhenni et al. (2007)).

- 200 1. We consider the preliminary estimate \hat{m} of m by the regression of Y_t on X_t with quadratic kernel
201 K , the semi-metric d_1^{PCA} and data driven bandwidth h_0^{opt} assuming i.i.d. errors (see Ferraty
202 and Vieu (2006) for more details):

$$h_0^{opt} = \arg \min_h \sum_{t=1}^T (Y_t - \hat{m}_{-t}(X_t))^2$$

203 where

$$\hat{m}_{-t}(x) = \frac{\sum_{u=1, u \neq t}^T Y_u K\left(\frac{d(x, X_u)}{h_0}\right)}{\sum_{s=1, s \neq t}^T K\left(\frac{d(x, X_s)}{h_0}\right)}$$

204 We calculate the estimated residuals $\hat{u}_t = Y_t - \hat{m}(X_t)$.

205 2. We conduct an estimation of the AR(1) coefficients in the autoregression of \hat{u}_t : $\hat{u}_t = \hat{a}_1 \hat{u}_{t-1} + \eta$,
 206 as in Section 2. We construct $\hat{Y}_t = Y_t - \hat{a}_1 (Y_{t-1} - \hat{m}(X_{t-1}))$, $t = 2, \dots, T$ and the estimate $\tilde{m}(x)$
 207 from the regression of \hat{Y}_t on X_t with quadratic kernel K , the semi-metric d_1^{PCA} and optimal
 208 data driven bandwidth h_1^{opt} in the same way as above, replacing $\hat{m}(x)$ by $\tilde{m}(x)$ resulting in:

$$h_1^{opt} = \arg \min_h \sum_{t=2}^T (Y_t - \tilde{m}_{-t}(X_t))^2.$$

209 The results in Table 1 show that there is great variability in the improvements across replica-
 210 tions. The inter-quartile ranges of the relative efficiencies are nevertheless tight: typically within
 211 0.1 – 0.2, except when the improvements are large (e.g. for $\rho = 0.9$). The mean improvements
 212 for the estimator is always smaller than 1 (i.e. showing a positive impact of our method) except
 213 when $\rho \leq 0.1$, a very small level of autocorrelation, where the values are 1.004 and 1.007, still very
 214 close to 1. The iterated estimator is much less efficient than the initial estimator. It seems that
 215 the additional steps are adding several layers of noise in the procedure and therefore degrade the
 216 estimation. Table 2 allows us to see the effect of sample size on the mean relative efficiency. It
 217 seems that such benefit is stronger whenever the autocorrelation is higher (as expected to be able to
 218 capture it properly). Moreover, for $\rho = 0.9, 0.6$ and 0.25 , three iterations have been implemented
 219 and the relative efficiency is still worst than at the first iteration and worst than at the second
 220 iteration. The results concerning these three iterations are given in Table 3.

Table 1: Elementary statistics of the relative efficiency for 2 iterations with $T = 200$

ρ	<i>RE</i>	<i>Min</i>	<i>Q₁</i>	<i>Med</i>	<i>Mean</i>	<i>Q₃</i>	<i>Max</i>
0.99	1	0.110	0.917	0.978	0.904	0.998	1.128
	2	0.116	0.928	0.982	0.941	1.033	1.564
0.95	1	0.068	0.702	0.883	0.813	0.966	1.111
	2	0.132	0.781	0.948	0.915	1.061	1.798
0.90	1	0.116	0.551	0.776	0.732	0.925	1.596
	2	0.120	0.737	0.897	0.925	1.093	2.766
0.80	1	0.251	0.669	0.782	0.797	0.941	1.568
	2	0.303	0.814	0.989	1.037	1.219	2.950
0.60	1	0.242	0.734	0.871	0.884	1.010	1.929
	2	0.271	0.921	1.080	1.144	1.277	3.270
0.50	1	0.393	0.804	0.909	0.921	1.049	1.463
	2	0.396	0.967	1.092	1.127	1.243	2.209
0.25	1	0.666	0.943	1.002	0.997	1.044	1.620
	2	0.580	0.971	1.037	1.055	1.113	1.777
0.10	1	0.822	0.977	1.001	1.007	1.028	1.436
	2	0.791	0.981	1.010	1.029	1.063	1.459
0.00	1	0.469	0.982	0.998	1.004	1.025	1.421
	2	0.466	0.972	1.004	1.008	1.033	1.555

Table 2: Mean of the relative efficiency for $T = 100, 200$ and 500 considering 2 iterations

T ρ	100		200		500	
	<i>RE1</i>	<i>RE2</i>	<i>RE1</i>	<i>RE2</i>	<i>RE1</i>	<i>RE2</i>
0.99	0.921	0.969	0.904	0.941	0.853	0.867
0.95	0.845	0.950	0.813	0.915	0.768	0.971
0.90	0.825	1.015	0.732	0.925	0.733	0.897
0.80	0.851	1.080	0.797	1.037	0.763	1.009
0.60	0.908	1.410	0.884	1.144	0.872	1.115
0.50	0.969	1.204	0.921	1.127	0.925	1.138
0.25	0.997	1.056	0.997	1.055	0.998	1.071
0.10	1.013	1.034	1.007	1.029	1.001	1.021
0.00	1.024	1.030	1.004	1.008	1.009	1.013

Table 3: Elementary statistics of the relative efficiency for 3 iterations with $T = 200$

ρ	<i>RE</i>	<i>Min</i>	Q_1	<i>Med</i>	<i>Mean</i>	Q_3	<i>Max</i>
0.90	1	0.116	0.551	0.777	0.731	0.924	1.590
	2	0.119	0.736	0.897	0.925	1.095	2.793
	3	0.151	0.755	0.967	1.005	1.212	2.708
0.60	1	0.241	0.736	0.873	0.884	1.010	1.929
	2	0.271	0.921	1.079	1.145	1.277	3.264
	3	0.536	0.997	1.182	1.233	1.390	4.019
0.25	1	0.666	0.943	1.001	0.996	1.042	1.619
	2	0.581	0.971	1.037	1.054	1.114	1.767
	3	0.591	0.980	1.049	1.074	1.135	1.697

221 The efficiencies for functional data seem better than for univariate time series (Xiao et al.
222 (2003)), although Xiao et al. (2003) considered an ARMA(1,1) case - and an AR(2) pre-whitening
223 - in their simulations that is more challenging (but in dimension one, not in infinite dimension
224 as here). Indeed in Xiao et al. (2003), the relative improvement was never below 0.85. Here,
225 we can reach average reductions below 0.75 for high correlation and long enough time series to
226 capture this high level of correlation accurately. According to Ferraty and Vieu (2006), the curse
227 of dimensionality, a well-known concept in nonparametric inference, does not affect functional data
228 with high correlation. This, combined with an appropriate choice of the semi-metric, can explain
229 the fact that the efficiencies seem better in functional context than univariate one. One illustration
230 is given in Figure 1: for one replication, considering $T = 200$ and a value of $\rho = 0.9$. The black curve
231 displays the true function $m(X_t)$, the blue curve corresponds to the standard kernel estimation
232 whereas the red and green curves correspond to the proposed estimator with one or two iterations
233 respectively. Note that in this case the common estimate of the curve is far from the true curve.
234 On the contrary, the curves obtained considering our methodology not only have the same shape as
235 the true curve but are very close to the truth. In this case, the information of the autocorrelation
236 function of the error process clearly improves the quality of the regression estimation. However,
237 when the autoregressive parameter is small, as expected, our methodology does not improve the
238 results obtained through the standard kernel procedure that does not account for correlation in the
239 errors. For example, Figure 2 shows the curves obtained considering $\rho = 0.25$ for one replication.
240 We cannot see large differences between the displayed curves. The three estimation curves are
241 close to the curve representing the true function. There is asymmetry in our regression fit, as we
242 can notice for instance that extremely low values are not well captured overall but the largest values

243 of the response are, and much more so by our method, especially in the case of high autocorrelation
 244 as shown in Figure 2 compare to Figure 1.

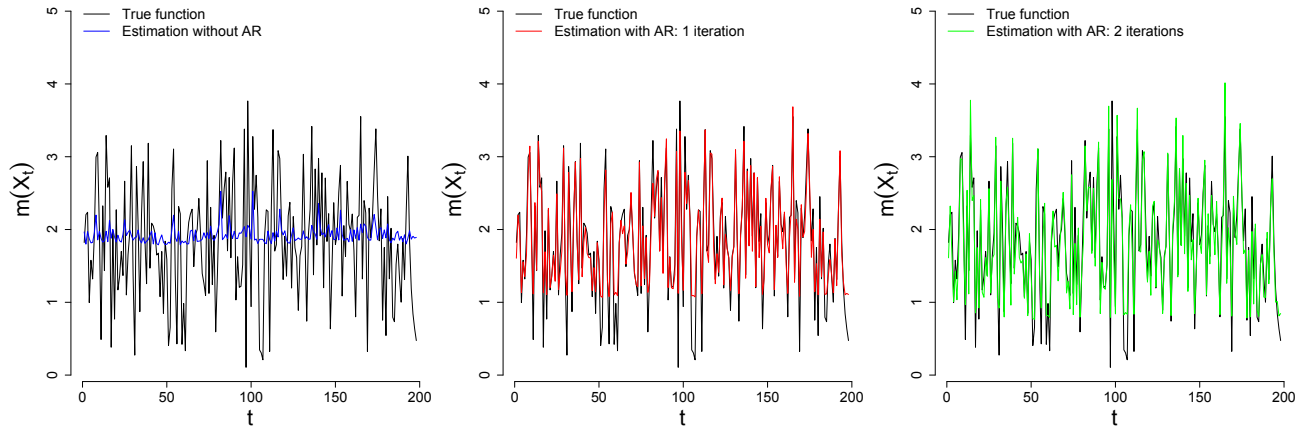


Figure 1: Estimates for $T = 200$ and $\rho = 0.9$. Black curve: true function $m(X_t)$, blue curve: standard kernel estimation, red and green curves: proposed estimator with one or two iterations respectively.

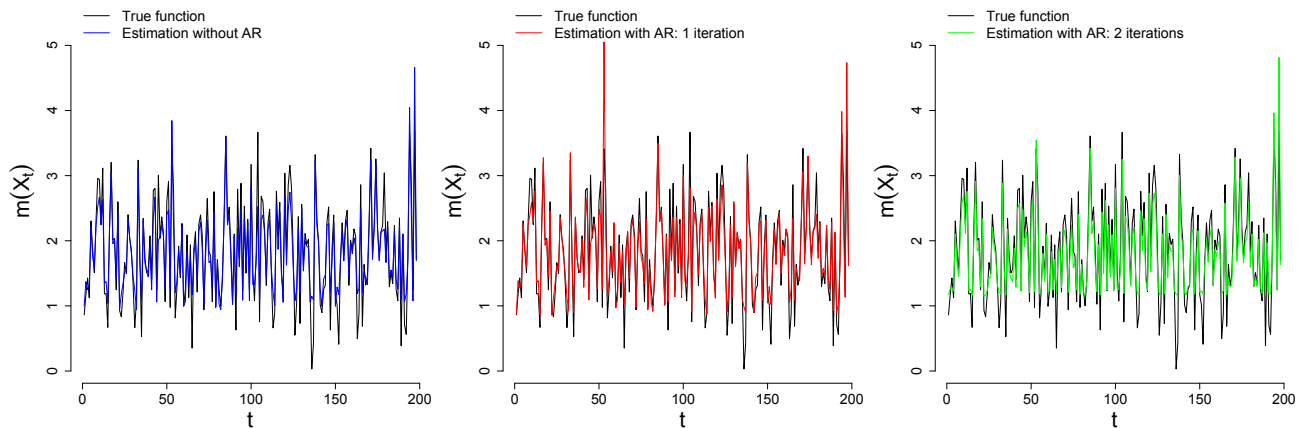


Figure 2: Estimates for $T = 200$ and $\rho = 0.25$. Black curve: true function $m(X_t)$, blue curve: standard kernel estimation, red and green curves: proposed estimator with one or two iterations respectively.

245 Some results are also obtained in environments with various levels of noise. Different values
 246 of the parameter σ from $\epsilon_t \sim \mathcal{N}(0, \sigma)$ have been tested. More precisely, different values of the
 247 signal-to-noise ratio (snr) have been considered where snr is defined as $Var(m(X_t))/\sigma^2$. The
 248 applied values are $snr = 1, 0.75, 0.5, 0.25$ and 0.05 . The obtained results are displayed in Table 4.
 249 We notice that when σ is higher, the relative efficiency is worse but for high autocorrelation our
 250 method still provides some improvements. For example, considering $\rho = 0.9$, the averaged $RE1$ is
 251 0.722 (resp. 0.748) with $\sigma = 0.77$ (resp. $\sigma = 3.42$).

252 We now present a challenging simulation in order to explore the robustness of our method in a

Table 4: Elementary statistics of the relative efficiency for $T = 200$ for different levels of signal-to-noise ratio considering 2 iterations

<i>snr</i>	<i>RE</i>	ρ	σ	<i>Min</i>	<i>Q₁</i>	<i>Med</i>	<i>Mean</i>	<i>Q₃</i>	<i>Max</i>	ρ	σ	<i>Min</i>	<i>Q₁</i>	<i>Med</i>	<i>Mean</i>	<i>Q₃</i>	<i>Max</i>
1.00	1	0.99	0.76	0.124	0.899	0.976	0.896	0.998	1.156	0.50	0.75	0.408	0.832	0.926	0.931	1.045	1.357
	2			0.156	0.921	0.981	0.938	1.032	1.608			0.494	0.990	1.122	1.175	1.310	3.215
0.75	1		0.87	0.116	0.905	0.977	0.899	0.998	1.156		0.87	0.398	0.821	0.921	0.929	1.046	1.499
	2			0.130	0.923	0.981	0.939	1.032	1.608			0.428	0.987	1.115	1.158	1.272	3.215
0.50	1		1.07	0.105	0.914	0.979	0.902	0.998	1.156		1.06	0.398	0.820	0.920	0.925	1.046	1.499
	2			0.105	0.926	0.983	0.940	1.032	1.608			0.362	0.975	1.108	1.144	1.259	3.215
0.25	1		1.51	0.091	0.921	0.981	0.907	0.100	1.156		1.50	0.329	0.813	0.920	0.925	1.047	1.707
	2			0.080	0.930	0.984	0.943	1.033	1.608			0.297	0.957	1.095	1.133	1.248	3.215
0.05	1		3.38	0.072	0.929	0.983	0.915	1.002	1.168		3.35	0.225	0.799	0.919	0.924	1.047	2.284
	2			0.053	0.930	0.985	0.949	1.034	1.826			0.297	0.938	1.081	1.119	1.244	3.504
1.00	1	0.95	0.82	0.073	0.699	0.869	0.809	0.967	1.222	0.25	0.83	0.716	0.950	1.002	0.995	1.042	1.538
	2			0.165	0.770	0.952	0.925	1.073	1.700			0.482	0.974	1.041	1.066	1.134	1.811
0.75	1		0.94	0.069	0.697	0.873	0.809	0.965	1.222		0.96	0.716	0.946	1.001	0.994	1.042	1.582
	2			0.141	0.766	0.950	0.920	1.071	1.756			0.482	0.973	1.037	1.064	1.132	1.945
0.50	1		1.15	0.056	0.704	0.873	0.811	0.967	1.222		1.18	0.716	0.947	1.001	0.995	1.041	1.651
	2			0.117	0.776	0.949	0.917	1.067	1.828			0.482	0.971	1.033	1.057	1.122	1.945
0.25	1		1.63	0.047	0.713	0.886	0.815	0.972	1.222		1.67	0.472	0.946	1.000	0.997	1.043	2.070
	2			0.093	0.769	0.949	0.915	1.069	1.828			0.482	0.968	1.033	1.052	1.121	1.945
0.05	1		3.65	0.038	0.734	0.908	0.829	0.982	1.946		3.73	0.232	0.942	0.999	1.002	1.046	2.452
	2			0.031	0.779	0.954	0.922	1.074	2.339			0.315	0.962	1.029	1.051	1.117	2.528
1.00	1	0.90	0.77	0.124	0.528	0.753	0.722	0.912	1.526	0.10	0.73	0.828	0.984	1.003	1.011	1.027	1.894
	2			0.146	0.768	0.927	0.966	1.129	3.603			0.787	0.985	1.011	1.036	1.067	1.927
0.75	1		0.88	0.122	0.534	0.760	0.723	0.913	1.571		0.84	0.756	0.981	1.003	1.009	1.027	1.894
	2			0.129	0.760	0.907	0.950	1.117	3.603			0.752	0.983	1.012	1.036	1.065	1.927
0.50	1		1.08	0.109	0.546	0.764	0.726	0.921	1.611		1.03	0.755	0.980	1.003	1.009	1.028	1.894
	2			0.123	0.753	0.899	0.937	1.100	3.603			0.752	0.983	1.011	1.035	1.065	1.927
0.25	1		1.53	0.091	0.550	0.772	0.733	0.928	1.611		1.46	0.755	0.977	1.002	1.008	1.029	1.894
	2			0.105	0.737	0.895	0.923	1.091	3.603			0.653	0.981	1.010	1.033	1.062	1.927
0.05	1		3.42	0.067	0.565	0.796	0.748	0.945	1.940		3.26	0.167	0.975	1.002	1.008	1.029	1.936
	2			0.105	0.737	0.898	0.920	1.094	3.603			0.599	0.979	1.010	1.032	1.063	2.135
1.00	1	0.80	0.79	0.223	0.665	0.818	0.807	0.961	1.536	0.00	0.82	0.362	0.985	0.999	1.000	1.019	1.262
	2			0.301	0.863	1.045	1.109	1.299	3.989			0.356	0.976	1.004	1.008	1.030	1.400
0.75	1		0.92	0.223	0.663	0.802	0.802	0.952	1.560		0.94	0.362	0.985	0.998	1.000	1.020	1.389
	2			0.292	0.846	1.025	1.079	1.267	3.989			0.356	0.973	1.003	1.008	1.031	1.523
0.50	1		1.12	0.223	0.663	0.797	0.801	0.948	1.566		1.16	0.362	0.983	0.998	1.000	1.019	1.389
	2			0.283	0.833	1.009	1.055	1.245	3.989			0.356	0.972	1.002	1.006	1.031	1.523
0.25	1		1.59	0.221	0.658	0.794	0.797	0.945	1.606		1.64	0.362	0.979	0.998	1.000	1.019	1.559
	2			0.283	0.802	0.990	1.034	1.219	3.989			0.356	0.972	1.002	1.006	1.032	1.523
0.05	1		3.55	0.189	0.662	0.813	0.806	0.958	1.828		3.66	0.362	0.978	0.998	1.003	1.022	2.777
	2			0.183	0.796	0.981	1.028	1.196	3.989			0.356	0.972	1.002	1.006	1.035	1.648
1.00	1	0.60	0.76	0.270	0.760	0.874	0.893	1.013	2.236								
	2			0.352	0.981	1.104	1.197	1.306	3.436								
0.75	1		0.88	0.250	0.757	0.876	0.889	1.011	2.236								
	2			0.296	0.959	1.100	1.177	1.296	3.436								
0.50	1		1.08	0.250	0.753	0.879	0.892	1.013	2.236								
	2			0.296	0.941	1.091	1.164	1.285	3.436								
0.25	1		1.53	0.250	0.743	0.875	0.892	1.015	2.236								
	2			0.296	0.926	1.074	1.147	1.265	3.571								
0.05	1		3.41	0.246	0.741	0.875	0.898	1.019	3.087								
	2			0.276	0.906	1.062	1.137	1.256	5.764								

253 more complex setting. The set-up is multivariate with bidimensional response (Y_1, Y_2) . First, the
254 functions X_t are still stationary (to satisfy the assumptions) but are now considered dependent.
255 Their dependence is introduced as an extension of the simple simulations with similar functional
256 observations as before: the X_t (with $t = 1, \dots, T$) are defined by $X_t(w) = 1 + 10e_{0,t} + 3e_{1,t}w^2 +$
257 $4e_{2,t}(1 - w)^3$, $w \in [0, 1]$ where $e_{0,t}$ and $e_{1,t}$ are i.i.d. $\mathcal{N}(0, 1)$, but now $e_{2,t}$ is an autoregressive
258 process $e_{2,t} = 0.9e_{2,t} + \epsilon_{t-1}^{(2)}$ where $\epsilon_t^{(2)}$ are i.i.d. $\mathcal{N}(0, 1)$. The two response functions are also more
259 complex, with a sinusoid integrated against the functional explanatory variable to provide further

260 nonlinear effects. We now take

$$m_1(X_t(w)) = m_2(X_t(w)) = 2\sqrt{\left|2 \int_0^1 X_t(w) \sin(\pi w) dw\right|}.$$

261 The error process \mathbf{u}_t is a $VAR(1)$ process, that is $\mathbf{u}_t: \mathbf{u}_t = \Pi_1 \mathbf{u}_{t-1} + \mathbf{e}_t$, where \mathbf{e}_t are i.i.d.
 262 $\mathcal{N}(0, \Sigma)$:

$$\Pi_1 = \begin{pmatrix} a & -0.3 \\ 0.1 & a/2 \end{pmatrix} \quad \Sigma = \begin{pmatrix} b & 0.8 \\ 0.8 & b/4 \end{pmatrix}$$

263 Various values of a and b are considered. The number of replications is 100. Table 5 presents
 264 the relative efficiencies with respect to a and b . The results show that the relative improvement can
 265 be as large as in the univariate case for more complex functions (and now including dependence
 266 in the explanatory variables). The case of a low autocorrelation level (0.25) demonstrates that
 267 the method still provides good results, equivalent to not taking into account the autocorrelation.
 268 When the autocorrelation is larger (e.g. 0.8-0.95), the results are typically best, as in the univariate
 269 case. For very high autocorrelation levels (e.g. 0.99), the relative efficiencies deteriorate slightly,
 270 due to the length of the series, as in the univariate case. The noise level seems to have a positive
 271 effect from 2 till 16 and then can possibly damage the efficiencies, especially for m_1 . Indeed, the
 272 noise needs to be large enough for the autocorrelation structure to be identified, and thus benefit
 273 the estimation, but not too high when it starts harming the estimation procedure. Nevertheless,
 274 even with a noise level 2-3 times higher than the optimal one, the efficiencies are relatively close
 275 to the optimal ones. Overall, the range of noise levels is large (from 1 to 24 times more), and the
 276 method shows resilience across the range.

277 3.2. Real data application

278 Here, we illustrate our methodology for the ozone concentration forecasting problem and com-
 279 pare our predictions with the ones obtained using the classical kernel regression model for functional
 280 data. The goal is to forecast ground-level ozone concentrations using observations from monitoring
 281 stations within the south-eastern US region, over a span of 3 months in the summer of 2005. These
 282 forecasts may contribute to better public health: for example, hourly forecasts made one day ahead
 283 of this harmful pollutant allow people avoid outdoor activities likely to damage their health.

284 We are given the ozone concentration for different stations for every hour from June 2 to August
 285 31, 2005 (that is 91 days). Since some of the stations had missing values, we use linear interpolation
 286 to estimate the missing values. We are interested in 1-day ahead ozone forecasting (specifically, r -
 287 hours ahead ozone forecasting, for $r = 1, \dots, 24$ that is, from 12am to 11pm). We have implemented
 288 the univariate and multivariate versions of our procedure, e.g. modeling the error term with an
 289 $AR(1)$ and with a $VAR(1)$. We denote the ozone concentration at time t by $Z(t)$ where t refers
 290 to the day and the hour of observation. We suppose that $Z(t)$ is observed for $t \in [1; 2160)$ (24

Table 5: Mean of relative efficiencies, bivariate model, 100 replications

		m_1				
		b	2	4	16	32
a	0.25	1.00	0.99	1.00	0.99	0.97
0.80	0.90	0.84	0.77	0.83	0.76	
0.90	0.83	0.79	0.74	0.78	0.79	
0.95	0.83	0.76	0.71	0.77	0.75	
0.99	0.82	0.78	0.77	0.79	0.77	

		m_2				
		b	2	4	16	32
a	0.25	0.99	0.98	0.93	0.88	0.89
0.80	0.94	0.89	0.79	0.75	0.73	
0.90	0.91	0.84	0.73	0.73	0.68	
0.95	0.88	0.81	0.69	0.69	0.72	
0.99	0.86	0.82	0.74	0.75	0.74	

291 hours \times 90 days) and we are interested in predicting $Z(2160 + r)$ for $r = 1, 2, \dots, 24$. In order to
 292 apply the functional methodology, we cut the original time series into a set of daily functional data.
 293 Here, we have decided to predict future ozone concentration by using the concentration data for
 294 the whole last day (24 hours). In order to illustrate our purpose, we will not use the 91th day and
 295 we will predict it by means of the data corresponding to the 90 previous ones. Then, as presented
 296 in Ferraty and Vieu (2006), for fixed r , the data will be reorganized into a functional explanatory
 sample $\{X_i, i = 1, \dots, 89\}$ which will be loaded in the following 89×24 matrix:

$Z(1)$	$Z(2)$	\dots	$Z(24)$
$Z(25)$	$Z(26)$	\dots	$Z(48)$
\vdots			
$Z(2113)$	$Z(2114)$	\dots	$Z(2136)$

297 and (for the univariate modeling) a response real sample $\{Y_i^{(r)}, i = 1, \dots, 89\}$, which will be loaded
 298 in the following 89-dimensional vector:

$Z(24 + r)$	$Z(48 + r)$	\dots	$Z(2136 + r)$
-------------	-------------	---------	---------------

299 For a fixed horizon r , we will predict the value of $Z(2160 + r)$. In the following, the predictions
 300 have been achieved for any value of $r = 1, 2, \dots, 24$. Note that in our procedure several parameters
 301 need to be selected. For the kernel, we use the quadratic one. Cross-validation methods, expressed
 302 in terms of k -nearest neighbours, are used for (local) smoothing parameter selection, see Chapter 7
 303 in Ferraty and Vieu (2006). Moreover, we use a semi-metric based on the first functional principal
 304 components of the data curves. For each considered situation, as in the previous simulation study,
 305 we have tested different values for the tuning parameter q . The following reported results come
 306

307 from a suitable choice of q , different according to the case. Finally, we proceed in the following
 308 way:

- 309 1. Select the horizon prediction r and organize the data as explained previously;
- 310 2. Predict $Y_{90}^{(r)}$, at fixed horizon r , by the classical kernel regression approach with a local choice
 311 of the number k of neighbors:

$$\hat{Y}_{90}^{(r)} = \hat{r}(X_{90}) = \frac{\sum_{i=1}^{89} Y_i^{(r)} K\left(\frac{d(X_i, X_{90})}{h_{k_{opt}(X_{i_0})}}\right)}{\sum_{i=1}^{89} K\left(\frac{d(X_i, X_{90})}{h_{k_{opt}(X_{i_0})}}\right)}$$

312 where $i_0 = \arg \min_{i=1, \dots, 89} d(X_{90}, X_i)$ and $h_{k_{opt}(X_{i_0})}$ is the bandwidth corresponding to the optimal
 313 number of neighbors at X_{i_0} obtained by

$$k_{opt}(X_{i_0}) = \arg \min_k \left| Y_{i_0} - \frac{\sum_{i=1, i \neq i_0}^n Y_i K\left(\frac{d(X_i, X_{i_0})}{h_k(X_{i_0})}\right)}{\sum_{i=1, i \neq i_0}^n K\left(\frac{d(X_i, X_{i_0})}{h_k(X_{i_0})}\right)} \right|$$

- 314 3. At step 2., during the learning step, the 89 response variables are estimated, denoted \hat{Y}_t ,
 315 $t = 1, \dots, 89$. Then, we construct the residual terms $\{\hat{u}_t\}$, where for $t = 1, \dots, 89$, $\hat{u}_t = Y_t - \hat{Y}_t$.
 316 We estimate the $AR(1)$ coefficient, a_1 , in the autoregression of \hat{u}_t .
- 317 4. Construct \tilde{Y}_t , $t = 2, \dots, 89$, as explained in Section 2, as an alternative to Step 2.

$$\tilde{Y}_{90}^{(r)} = \tilde{r}(X_{90}) = \frac{\sum_{i=2}^{89} \tilde{Y}_i^{(r)} K\left(\frac{d(X_i, X_{90})}{h_{k_{opt}(X_{i_0})}}\right)}{\sum_{i=2}^{89} K\left(\frac{d(X_i, X_{90})}{h_{k_{opt}(X_{i_0})}}\right)}$$

318 We apply the previous procedure on Station 20 to predict ozone on August 31st, the 91st
 319 day. The series of observations are represented in the left panel of Figure 3. On the right panel
 320 of this figure, the daily curves are plotted in grey and the black curve represents the curve we
 321 want to forecast. The results obtained at Step 2. (by the classical kernel method) are displayed
 322 in blue whereas those of Step 4. considering an $AR(1)$ (from our procedure presented in Section
 323 2) are displayed in red. From this figure, one can observe that our method improves upon the
 324 results obtained with the classical method, in particular for the second half of the day. In fact, the
 325 estimated coefficients in the autoregression of \hat{u}_i are higher for that part of the day, see Table 6. The
 326 figures of ACFs (autocorrelation functions) and PACFs (partial autocorrelation functions) show
 327 that there is insignificant autocorrelation in the errors, except from 11am ($r = 12$) to 16pm ($r = 17$)
 328 where an $AR(1)$ would be the best fit. Hence, using our approach for these hours is justified. We
 329 even use our approach for all the hours of the day since there is only a tiny loss by doing so when
 330 there is very little autocorrelation. We notice in Figure 3 that the forecasts using our method are

331 much closer to observations over the afternoon (11am till 16am) compared to the i.i.d. regression,
 332 when the benefit of our approach is indeed maximized. Figure 4 displays autocorrelation and partial
 333 autocorrelation functions for some horizons r ($r = 6, 12, 17$ and 21). The bold character in Table
 334 6 is used to emphasize horizons for which the corresponding autocorrelation function justifies an
 335 $AR(1)$. In addition, we compute the mean squared errors (MSE) to compare the results obtained
 336 by the different methods. For Station 20, the MSE from the classical approach is 159.91 whereas
 337 with our approach it is reduced to 126.3. The corresponding relative efficiency is 0.79. Again we
 338 note that the fact of taking into account the autocorrelation in the error process allows to improve
 339 ozone forecasting.

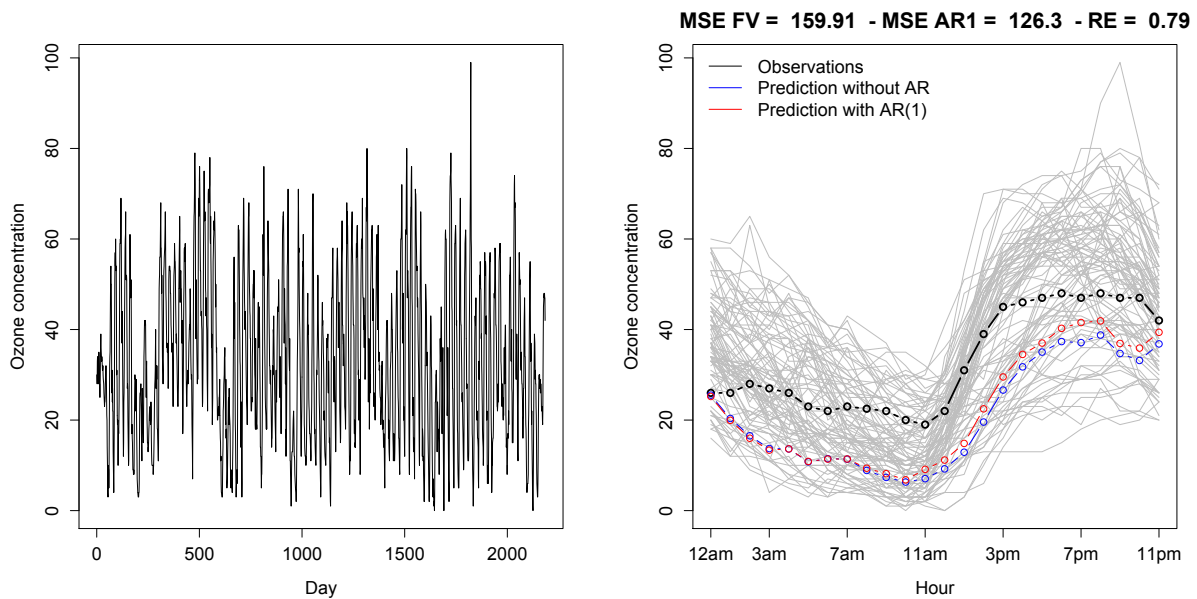


Figure 3: Ozone concentrations and predictions considering an $AR(1)$ modeling of the error term at Station 20
 Left: all the series. Right: predictions.

Table 6: Station 20: for horizon predictions r , estimated autoregressive coefficients \hat{a}_1

r	1	2	3	4	5	6	7	8	9	10	11	12
\hat{a}_1	-0.06	-0.13	-0.13	-0.14	0.01	0.02	-0.02	0.01	0.12	0.18	0.12	0.30
r	13	14	15	16	17	18	19	20	21	22	23	24
\hat{a}_1	0.33	0.22	0.30	0.27	0.25	0.19	0.18	0.16	0.08	0.12	0.16	0.17

340 Now, we present results obtained considering the multivariate extension. Instead of fixing the
 341 horizon r and repeating the procedure for all the horizons to study, we predict all the period in
 342 one implementation. We construct the 89 vectors \mathbf{Y}_t in the following way. For $t = 1, \dots, 89$,

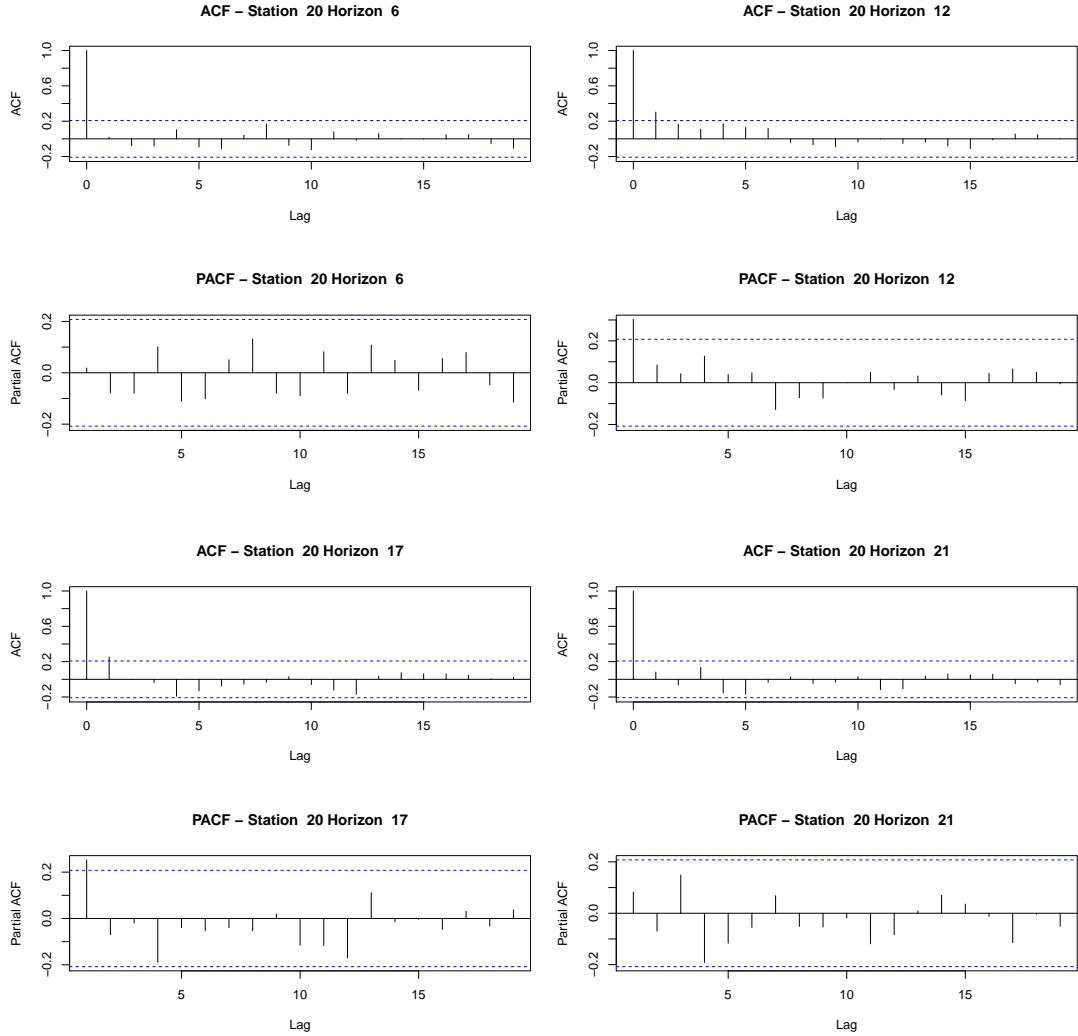


Figure 4: Autocorrelation and partial autocorrelation functions (acf and pacf) at Station 20, for $r = 6, 12, 17, 21$.

$$\begin{aligned} \mathbf{Y}_t &= (Y_{t,1}, \dots, Y_{t,24})' \\ &= \left(Z(24 \times t + 1) \quad Z(24 \times t + 2) \quad \dots \quad Z(24 \times t + 24) \right)' \end{aligned}$$

343 The estimation procedure is similar to the univariate case, the main change appears in the
 344 error modeling. In this illustration, we estimate the $VAR(1)$ coefficients of $\hat{\mathbf{u}}_t$. We proceed in the
 345 following way:

- 346 1. For $j = 1, \dots, 24$, predict $Y_{90,j}$ by the classical kernel regression approach with a local choice

347 of the number k of neighbors:

$$\widehat{Y}_{90,j} = \widehat{r}(X_{90}) = \frac{\sum_{i=1}^{89} Y_{i,j} K\left(\frac{d(X_i, X_{90})}{h_{k_{opt}(X_{i_0})}}\right)}{\sum_{i=1}^{89} K\left(\frac{d(X_i, X_{90})}{h_{k_{opt}(X_{i_0})}}\right)}$$

348 where $i_0 = \arg \min_{i=1, \dots, 89} d(X_{90}, X_i)$ and $h_{k_{opt}(X_{i_0})}$ is the bandwidth corresponding to the optimal
 349 number of neighbors at X_{i_0} .

- 350 2. At step 1., during the learning step, the 89 vectors are estimated, denoted $\widehat{\mathbf{Y}}_t$, $t = 1, \dots, 89$.
 351 Then, we construct the residual terms $\{\widehat{\mathbf{u}}_t\}$, where for $t = 1, \dots, 89$, $\widehat{\mathbf{u}}_t = \mathbf{Y}_t - \widehat{\mathbf{Y}}_t$. We
 352 estimate the $VAR(1)$ coefficients, Π_1 , in the autoregression of $\widehat{\mathbf{u}}_t$.
 353 3. Construct $\widehat{\mathbf{Y}}_t$, $t = 2, \dots, 89$, as explained in Section 2, as an alternative to Step 1, we have

$$\widetilde{Y}_{90,j} = \widetilde{r}(X_{90}) = \frac{\sum_{i=2}^{89} \widehat{Y}_{i,j} K\left(\frac{d(X_i, X_{90})}{h_{k_{opt}(X_{i_0})}}\right)}{\sum_{i=2}^{89} K\left(\frac{d(X_i, X_{90})}{h_{k_{opt}(X_{i_0})}}\right)}$$

354 As it is done previously, we apply this multivariate procedure on Station 20 to predict ozone on
 355 August 31st, the 91st day. On Figure 5, the daily curves are plotted in grey and the black curve
 356 represents the curve we want to forecast. The results obtained at Step 1 (by the classical kernel
 357 method) are displayed in blue whereas those of Step 3 considering a $VAR(1)$ (from our procedure
 358 presented in Section 2) are displayed in red. Note that the results obtained with the classical
 359 method are similar to the univariate case. From this figure, one can observe that our method
 360 again improves upon the results obtained with the classical method. The MSE is 85.25 and the
 361 corresponding relative efficiency is 0.53 which is much better than using the univariate modeling
 362 of the error term.

363 To conclude, the case study shows that using our methodology can improve the ozone con-
 364 centration predictions obtained with the classical kernel regression estimate. Neighboring stations
 365 should contain additional information on each other. A joint modeling is possible, as shown in
 366 Ettinger et al. (2012). Time series of random surfaces at one particular hour of ozone are used in
 367 that paper to predict a particular hour at one location the day after. It was shown there that this
 368 approach of borrowing strength across space compares favorably to using the whole series of times
 369 (i.e. a curve) over the previous day to predict the future values a particular hour at one location
 370 the day after.

371 4. Conclusion

372 We have developed a two-stage procedure in order to estimate a nonlinear functional regression
 373 where the explanatory variable is functional and the residual process is stationary and autocor-

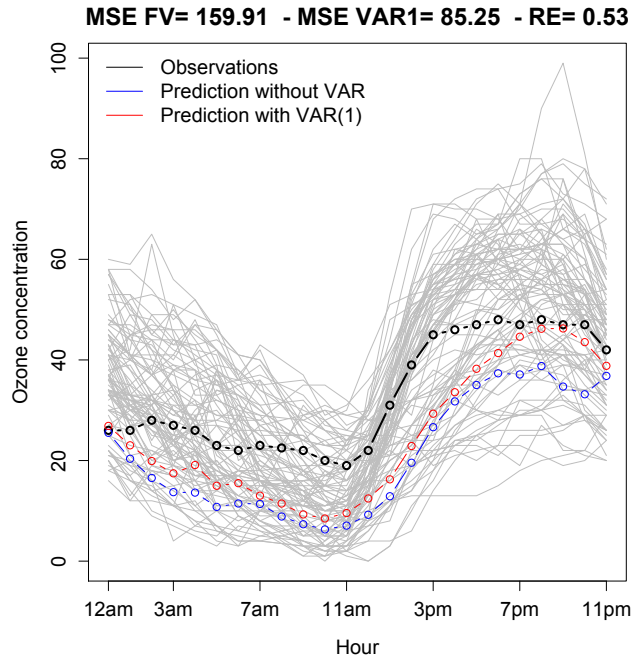


Figure 5: Ozone concentrations and predictions at Station 20 considering a $VAR(1)$ modeling of the error term

374 related. We have considered the case where the response variable is valued in \mathbb{R}^d , $d \geq 1$. This
 375 constitutes, to our knowledge a first step in the research on functional nonparametric modeling
 376 with a multivariate response. We have used the information of the autocorrelation function of the
 377 error process to improve the kernel-based estimation of the regression function. The asymptotic
 378 normality of our estimator is proved under some conditions. Some numerical results from a simu-
 379 lation case study and an application on real data illustrate the benefit of using this approach. Our
 380 methodology improves the standard kernel estimator in presence of highly autocorrelated data.

381 Potential improvements relate to the optimal implementation of our method. Indeed, the
 382 numerical illustrations indicate that there is a “sweet spot” where the number of time points
 383 provide enough information relative to the autocorrelation level to allow an optimal reduction of the
 384 prediction error. Another aspect is that for small autocorrelation levels, our approach deteriorates
 385 slightly the prediction errors compared to the use of independence-based kernel methods. An
 386 improved method should account for that fact and revert back to the basic independence-based
 387 kernel methods in these regimes.

388 Besides, in the literature on regression estimation with functional predictors, nonparameric
 389 methods with a Nadaraya-Watson-type estimator are successfully used. However, some authors
 390 proposed instead to use semi-parametric models which are shown to be interesting alternatives.
 391 For example, we could deal with functional partial linear model (see e.g. Aneiros-Pérez and Vieu
 392 (2008), Dabo-Niang and Guillas (2010)), functional index model (see e.g. Chen et al. (2011)),

393 or with functional projection pursuit regression (see e.g. Ferraty et al. (2013)). These kind of
394 alternatives to fully non-parametric models are beyond the scope of this work but will be the aim
395 of futur investigations. In this further work, our procedure taking into account the autocorrelation
396 in the error term could be adapted in the more general framework of functional index models (Chen
397 et al. (2011)). More precisely, we could place a linear model inside a link function. We could first
398 estimate the parameters of the linear model using least squares methodology. Secondly, the link
399 function could be estimated non parametrically including our two-stage procedure.

400 Finally, our approach could be extended to other time series of functional data. Aue et al.
401 (2015) recently provided a dimension reduction technique with functional principal components
402 (FPC) analysis that enables the use of vector-valued time series of FPC scores. However, this
403 model did not allow of autocorrelation in the residuals that can still be present as we show in
404 our ozone application above. A combination of the two approaches and that of Aue et al. (2014),
405 that provided fully functional regression models allowing for autocorrelated errors, would have the
406 potential to further improve the quality of predictions.

407 5. Appendix: Proofs of Theorems

408 We use C to signify a generic positive constant whose exact value may vary from case to case.
409

Lemma 1. *Under assumptions **H1-H5** (or more precisely **H1, H2, H3(1), H3(2), H4, H5**)*

$$(T\phi(h_0))^{1/2} [\bar{\mathbf{m}}(x) - \mathbf{m}(x) - \mathbf{B}_T^*(x)] \xrightarrow{d} \mathcal{N}_d(0, \Sigma_x)$$

410 with $\Sigma_x = \frac{C_2 \mathbf{G}_2(x)}{C_1^2 f_1(x)}$ is the $(d \times d)$ asymptotic covariance matrix with elements, $x \in (\mathcal{C}, d)$ whenever
411 $f_1(x) > 0$, and $\mathbf{B}_T^*(x) = \mathbb{E}[\bar{\mathbf{m}}(x)] - \mathbf{m}(x)$.

412 Lemma 1 comes from Theorem 5 in Masry (2005). The functions $\mathbf{G}_2(x)$, $f_1(x)$ and $\phi(h_0)$ are given
413 in assumptions **H1** and **H3**.

414 **Remark 3.** *As stated in Masry (2005), if in addition to the assumptions of Lemma 1 we have*
415 $T\phi(h_0)h_0^{2\beta} \rightarrow 0$ *(it is a stronger assumption on the bandwidth parameter) then one can remove the*
416 *bias term from Lemma 1 that is $(T\phi(h_0))^{1/2} [\bar{\mathbf{m}}(x) - \mathbf{m}(x)] \xrightarrow{d} \mathcal{N}_d(0, \Sigma_x)$.*

417 5.1. Proof of Lemma 1

The proof follows work of Masry (2005). We make use of the Cramér-Wold device (see, e.g. Van der Vaart (1998), p.16), according to which it is sufficient to prove that for all $\mathbf{v} \in \mathbb{R}^d$, $\|\mathbf{v}\| \neq 0$, we have

$$(T\phi(h_0))^{1/2} [\mathbf{v}' (\bar{\mathbf{m}}(x) - \mathbf{m}(x) - \mathbf{B}_T^*(x))] \xrightarrow{d} \mathcal{N}_d(0, \mathbf{v}' \Sigma_x \mathbf{v})$$

Note that $\mathbf{Y}_t = \mathbf{m}(X_t) + \mathbf{e}_t$; $\mathbf{v}'(\bar{\mathbf{m}}(x) - \mathbf{m}(x)) = (\bar{m}_{\mathbf{v}}(x) - m_{\mathbf{v}}(x))$, where

$$\bar{m}_{\mathbf{v}}(x) = \frac{\frac{1}{T\mathbb{E}\left[K_0\left(\frac{d(x, X_1)}{h_0}\right)\right]} \sum_{t=1}^T \mathbf{v}'\mathbf{Y}_t K_0\left(\frac{d(x, X_t)}{h_0}\right)}{\frac{1}{T\mathbb{E}\left[K_0\left(\frac{d(x, X_1)}{h_0}\right)\right]} \sum_{s=1}^T K_0\left(\frac{d(x, X_s)}{h_0}\right)} = \frac{\bar{m}_{2\mathbf{v}}(x)}{\bar{m}_1(x)}, \quad m_{\mathbf{v}}(x) = \mathbf{v}'m(x).$$

Then, we obtain $\bar{m}_{\mathbf{v}}(x) = m_{\mathbf{v}}(x) + B_T^{\mathbf{v}}(x) + V_T^{\mathbf{v}}(x)$ where $B_T^{\mathbf{v}}(x)$ is the bias term and $V_T^{\mathbf{v}}(x)$ is the variance effect defined by

$$B_T^{\mathbf{v}}(x) = \frac{\mathbb{E}[\bar{m}_{2\mathbf{v}}(x)] - m_{\mathbf{v}}(x)\mathbb{E}[\bar{m}_1(x)]}{\mathbb{E}[\bar{m}_1(x)]} \quad V_T^{\mathbf{v}}(x) = \frac{Q_T^{\mathbf{v}}(x) - B_T^{\mathbf{v}}(x)(\bar{m}_1(x) - \mathbb{E}[\bar{m}_1(x)])}{\bar{m}_1(x)}$$

with $Q_T^{\mathbf{v}}(x) = (\bar{m}_{2\mathbf{v}}(x) - \mathbb{E}[\bar{m}_{2\mathbf{v}}(x)]) - m_{\mathbf{v}}(x)(\bar{m}_1(x) - \mathbb{E}[\bar{m}_1(x)])$. By the result of Masry (2005), $B_T^{\mathbf{v}}(x) = o(h_0^\beta)$ and using same lines as in the proof of Theorem 5 in Masry (2005), we have

$$(T\phi(h_0))^{1/2} [\mathbf{v}'(\bar{\mathbf{m}}(x) - \mathbf{m}(x) - \mathbf{B}_T^*(x))] \xrightarrow{d} \mathcal{N}_d(0, \mathbf{v}'\Sigma_x\mathbf{v}).$$

418 5.2. Proof of Theorem 1

$$\text{We have } \tilde{\mathbf{m}}(x) = \frac{\frac{1}{T\mathbb{E}[\Delta_1^{(1)}(x)]} \sum_{t=1}^T \hat{\mathbf{Y}}_t \Delta_t^{(1)}(x)}{\frac{1}{T\mathbb{E}[\Delta_1^{(1)}(x)]} \sum_{t=1}^T \Delta_t^{(1)}(x)} = \frac{\tilde{\mathbf{m}}_2(x)}{\tilde{m}_1(x)}, \quad \tilde{\mathbf{m}}_2(x) = (\tilde{m}_{1,2}(x), \dots, \tilde{m}_{d,2}(x))'$$

where

$$\tilde{m}_{j,2}(x) = \frac{1}{T\mathbb{E}[\Delta_1^{(1)}(x)]} \sum_{t=1}^T \hat{Y}_{t,j} \Delta_t^{(1)}(x), \quad j = 1, \dots, d$$

$$\tilde{m}_1(x) = \frac{1}{T\mathbb{E}[\Delta_1^{(1)}(x)]} \sum_{t=1}^T \Delta_t^{(1)}(x)$$

$$\begin{aligned} \sum_{t=1}^T \hat{Y}_{t,j} \Delta_t^{(1)}(x) &= \sum_{t=1}^T Y_{t,j} \Delta_t^{(1)}(x) - \sum_{t=1}^T \left[(\hat{\Pi}_1 - \Pi_1) u_{t-1} \right]_j \Delta_t^{(1)}(x) + \sum_{t=1}^T [\Pi_1 (\hat{\mathbf{m}}(X_{t-1}) - \mathbf{m}(X_{t-1}))]_j \Delta_t^{(1)}(x) \\ &\quad + \sum_{t=1}^T \left[(\hat{\Pi}_1 - \Pi_1) (\hat{\mathbf{m}}(X_{t-1}) - \mathbf{m}(X_{t-1})) \right]_j \Delta_t^{(1)}(x) \end{aligned}$$

Then $\tilde{m}_{j,2}(x) = \bar{m}_{j,2}(x)^\sharp - \tilde{m}_{j,21}(x) + \tilde{m}_{j,22}(x) + \tilde{m}_{j,23}(x)$ with

$$\begin{aligned}\bar{m}_{j,2}(x)^\sharp &= \frac{1}{T\mathbb{E}[\Delta_t^{(1)}(x)]} \sum_{t=1}^T Y_{t,j} \Delta_t^{(1)}(x) \\ \tilde{m}_{j,21}(x) &= \frac{1}{T\mathbb{E}[\Delta_t^{(1)}(x)]} \sum_{t=1}^T [(\hat{\Pi}_1 - \Pi_1) u_{t-1}]_j \Delta_t^{(1)}(x) \\ \tilde{m}_{j,22}(x) &= \frac{1}{T\mathbb{E}[\Delta_t^{(1)}(x)]} \sum_{t=1}^T [\Pi_1 (\hat{\mathbf{m}}(X_{t-1}) - \mathbf{m}(X_{t-1}))]_j \Delta_t^{(1)}(x) \\ \tilde{m}_{j,23}(x) &= \frac{1}{T\mathbb{E}[\Delta_t^{(1)}(x)]} \sum_{t=1}^T [(\hat{\Pi}_1 - \Pi_1) (\hat{\mathbf{m}}(X_{t-1}) - \mathbf{m}(X_{t-1}))]_j \Delta_t^{(1)}(x)\end{aligned}$$

419 Note that $\bar{m}_{j,2}(x)^\sharp = \bar{m}_{j,2}(x)$ and $\tilde{m}_1(x) = \bar{m}_1(x)$ with K_0 and h_0 replaced by K_1 and h_1 re-
 420 spectively. Since $\tilde{m}_j(x) = \frac{\tilde{m}_{j,2}(x)}{\tilde{m}_1(x)}$ we have $\tilde{\mathbf{m}}(x) = \bar{\mathbf{m}}(x) - Q_{T_1} + Q_{T_2} + Q_{T_3}$ with $Q_{T_l} =$
 421 $(Q_{1,T_l}, \dots, Q_{d,T_l})$, with $Q_{j,T_l} = \frac{\tilde{m}_{j,2l}(x)}{\tilde{m}_1(x)}$, for $l = 1, 2, 3$, $j = 1, \dots, d$. We analyze the asymp-
 422 totic properties of Q_{j,T_l} , $l = 1, 2, 3$, in Lemmas 2, 3 and 4, which are key results for proof of this
 423 theorem since Lemma 1 proves the asymptotic normality of $\bar{\mathbf{m}}(x)$.

424 **Lemma 2.** Under assumptions **H1-H5**, for $j = 1, \dots, d$, we have $Q_{j,T_1} = o_p\left(\sqrt{\frac{1}{T\phi(h_1)}}\right)$.

425 **Lemma 3.** Under assumptions **H1-H4**, for $j = 1, \dots, d$, we have $Q_{j,T_2} = O_p\left(h_0^\beta\right) + o_p\left(\sqrt{\frac{1}{T\phi(h_1)}}\right)$.

426 **Lemma 4.** Under assumptions **H1-H5**, for $j = 1, \dots, d$, we have $Q_{j,T_3} = O_p\left(h_0^\beta\right) + o_p\left(\sqrt{\frac{1}{T\phi(h_1)}}\right)$.

427 The proofs of Lemmas 2, 3 and 4 are given in the supplementary file.

428 *Proof of Theorem 2*

429 The proof is similar to that of Theorem 1 since $\tilde{m}_j(x) = \bar{m}_j(x) - Q_{j,T_1} + Q_{j,T_2} + Q_{j,T_3}$ with
 430 $Q_{j,T_l} = \frac{\tilde{m}_{j,2l}(x)}{\tilde{m}_1(x)}$, for $l = 1, 2, 3$, $j = 1, \dots, d$. It then follows directly from Corollary 1 of Masry
 431 (2005), Lemmas 2, 3 and 4, which are key results for proof of this theorem.

- 432 Aneiros-Pérez, G., Vieu, P., 2008. Nonparametric time series prediction: A semi-functional partial linear modeling.
 433 Journal of Multivariate Analysis 99, 834–857.
 434 Antoniadis, A., Brossat, X., Cugliari, J., Poggi, J.M., 2014. Une approche fonctionnelle pour la prévision non-
 435 paramétrique de la consommation d'électricité. Journal de la Société Française de Statistique 155, 202–219.
 436 Aston, J.A., Chiou, J.M., Evans, J.P., 2010. Linguistic pitch analysis using functional principal component mixed
 437 effect models. J. R. Stat. Soc. Ser. C. Appl. Stat. 59, 297–317.
 438 Aue, A., Hormann, S., Horváth, L., Huvsková, M., 2014. Dependent functional linear models with applications to
 439 monitoring structural change. Statistica Sinica 24, 1043–1073.
 440 Aue, A., Norinho, D.D., Hormann, S., 2015. On the prediction of stationary functional time series. Journal of the
 441 American Statistical Association 110.
 442 Benhenni, K., Ferraty, F., Rachdi, M., Vieu, P., 2007. Local smoothing regression with functional data. Computa-
 443 tional Statistics 22, 353–369.

- 444 Chen, D., Hall, P., Müller, H.G., et al., 2011. Single and multiple index functional regression models with nonpara-
445 metric link. *The Annals of Statistics* 39, 1720–1747.
- 446 Cuevas, A., 2014. A partial overview of the theory of statistics with functional data. *J. Statist. Plann. Inference* 147,
447 1–23.
- 448 Dabo-Niang, S., 2004. Kernel density estimator in an infinite-dimensional space with a rate of convergence in the
449 case of diffusion process. *Appl. Math. Lett.* 17, 381–386.
- 450 Dabo-Niang, S., Guillas, S., 2010. Functional semiparametric partially linear model with autoregressive errors.
451 *Journal of Multivariate Analysis* 101, 307–315.
- 452 Dabo-Niang, S., Rhomari, N., 2009. Kernel regression estimation in a banach space. *J. Statist. Plann. Inference* 139,
453 1421–1434.
- 454 Delsol, L., 2007. CLT and L_q errors in nonparametric functional regression. *C. R. Math. Acad. Sci.* 345, 411–414.
- 455 Delsol, L., 2009. Advances on asymptotic normality in non-parametric functional time series analysis. *Statistics* 43,
456 13–33.
- 457 Ettlinger, B., Guillas, S., Lai, M.J., 2012. Bivariate splines for ozone concentration forecasting. *Environmetrics* 23,
458 317–328.
- 459 Ferraty, F., Goia, A., Salinelli, E., Vieu, P., 2013. Functional projection pursuit regression. *Test* 22, 293–320.
- 460 Ferraty, F., Goia, A., Vieu, P., 2002a. Functional nonparametric model for time series : a fractal approach for
461 dimension reduction. *Test* 11, 317–344.
- 462 Ferraty, F., Goia, A., Vieu, P., 2002b. Régression non-paramétrique pour des variables aléatoires fonctionnelles
463 mélangées. *C. R. Math. Acad. Sci. Paris* 334, 217–220.
- 464 Ferraty, F., Mas, A., Vieu, P., 2007. Advances on nonparametric regression for functional data. *Aust. N. Z. J. Stat.*
465 49, 267–286.
- 466 Ferraty, F., Vieu, P., 2002. The functional nonparametric model and application to spectrometric data. *Comput.*
467 *Statist.* 17, 545–564.
- 468 Ferraty, F., Vieu, P., 2004. Nonparametric models for functional data, with application in regression, time series
469 prediction and curve discrimination. *J. Nonparametr. Stat.* 16, 111–125.
- 470 Ferraty, F., Vieu, P., 2006. *Nonparametric functional data analysis: theory and practice*. Springer.
- 471 Gasser, T., Hall, P., Presnell, B., 1998. Nonparametric estimation of the mode of a distribution of random curves.
472 *J. R. Stat. Soc. Ser. B Stat. Methodol.* 60, 681–691.
- 473 Guillas, S., Lai, M.J., 2010. Bivariate splines for spatial functional regression models. *J. Nonparametr. Stat.* 22,
474 477–497.
- 475 Härdle, W., Marron, J.S., 1985. Optimal bandwidth selection in nonparametric regression function estimation. *The*
476 *Annals of Statistics* , 1465–1481.
- 477 Hart, J.D., Vieu, P., 1990. Data-driven bandwidth choice for density estimation based on dependent data. *The*
478 *Annals of Statistics* , 873–890.
- 479 Lin, X., Carroll, R.J., 2000. Nonparametric function estimation for clustered data when the predictor is measured
480 without/with error. *Journal of the American statistical Association* 95, 520–534.
- 481 Masry, E., 2005. Nonparametric regression estimation for dependent functional data: asymptotic normality. *Stochas-*
482 *tic Process. Appl.* 115, 155–177.
- 483 Ogden, R.T., Greene, E., 2010. Wavelet modeling of functional random effects with application to human vision
484 data. *J. Statist. Plann. Inference* 140, 3797–3808.
- 485 Park, A., Guillas, S., Petropavlovskikh, I., 2013. Trends in stratospheric ozone profiles using functional mixed models.
486 *Atmospheric Chemistry and Physics* 13, 11473–11501.
- 487 Rachdi, M., Vieu, P., 2007. Nonparametric regression for functional data: Automatic smoothing parameter selection.
488 *Journal of Statistical Planning and Inference* 137, 2784–2801.
- 489 Ramsay, J., Silverman, B., 2005. *Functional data analysis*. 2nd ed., Springer.
- 490 Rosenblatt, M., 1956. A central limit theorem and a strong mixing condition. *Proceedings of the National Academy*
491 *of Sciences of the United States of America* 42, 43.
- 492 Ruckstuhl, A., Welsh, A., Carroll, R.J., 2000. Nonparametric function estimation of the relationship between two
493 repeatedly measured variables. *Statist. Sinica* 10, 51–71.
- 494 Sangalli, L.M., Ramsay, J.O., Ramsay, T.O., 2013. Spatial spline regression models. *Journal of the Royal Statistical*
495 *Society: Series B (Statistical Methodology)* 75, 681–703.
- 496 Van der Vaart, A., 1998. *Asymptotic Statistics*. volume 3. Cambridge University Press.
- 497 Xiang, D., Qiu, P., Pu, X., 2013. Nonparametric regression analysis of multivariate longitudinal data. *Statistica*
498 *Sinica* 23, 769–789.
- 499 Xiao, Z., Linton, O., Carroll, R., Mammen, E., 2003. More efficient local polynomial estimation in nonparametric

500 regression with autocorrelated errors. *J. Amer. Statist. Assoc.* 98, 980–992.